

Geometry-discrete load measurement on a cultivator tool

Johannes Bührke, Florian Schramm, Ludger Frerichs

For the validation of analytical and numerical calculations of soil-mechanical processes in agricultural engineering, detailed information from experiments is required. A new type of measuring system for recording geometric discrete partial forces on a cultivator tool is presented. The influences of the process parameters working depth and working speed were investigated within reproducible tests in a soil bin. The results show the qualitative and quantitative relationships of the process parameters on partial and total forces at the analysed tool. In addition, an approach for extrapolating the measured partial loads onto geometry sections of the measuring tool not covered by measurement equipment is presented and evaluated. Hence, force progression over the geometry sections of a cultivator tool can be described in more detail. This new type of detailed information serves to validate calculations and is therefore the basis for wear and tear or other process investigations.

Keywords

Metrological load profile, geometric discrete tool loading, agricultural soil mechanics, soil resistance, cultivator tines

The reasons for dealing with agricultural soil mechanics, which is particularly influenced by SÖHNE (1956), have remained unchanged despite the knowledge and state of technology that has grown over the years:

- a detailed understanding of the processes involved in the interaction of machine and soil,
- research of physical properties of agricultural soils, occurring forces, stresses and deformations of the agricultural soil under the influences of machines and
- the application of these findings to the design of agricultural machines.

Computation-intensive simulation methods, such as finite or discrete element methods are widely used in science and technology. However, spread of these methods and tools is rather different. Thus, the structural design of machines can be investigated relatively well with the help of Finite Element Methods (FEM) and is widespread in application. Whereas the investigation and application of the Discrete Elements Methods (DEM), in the context of agricultural soil mechanics, is much less done. In order to make greater use of the promising potential of agricultural soil simulation, further detailed investigations of the complex interaction characteristics of soil are required. Approaches such as those of UCGUL et al. (2014) show a current status of this research.

The objective of current investigations at the Institute for Mobile Machines and Commercial Vehicles in Braunschweig is to generate detailed knowledge of the processes involved in the operation of tools in the soil. Using a cultivator tool as an example, the respective processes are investigated and the further development of the simulation method is carried out in parallel. The parameters are determined and validated with a new type of load measurement during real working processes.

The measurement of loads on agricultural soil tillage tools is a common approach for the investigation of soil-mechanical fracturing, flow or friction processes. Researchers in the 1950s and 60s, for example, investigated the fundamental breaking-up forms of different soils or the influence of tool dimensions (angle of attack, tool width) on soil resistance (SÖHNE 1956, SIEMENS et al. 1965, VORNKAHL 1967). These investigations were based on draught and vertical force measurements of the total forces acting on the tool. There was no detailed differentiation of forces acting in different areas of the tool. Nevertheless, SÖHNE (1956) showed a two-dimensional theoretical approach to calculate the reaction forces of the soil on a curved surface.

For measuring partial loads on soil tillage tools, pressure measurements were carried out at selected points of a plough body (MATTETTI et al. 2015). Investigations by the AREEO (Agricultural Research Education and Extension Organization) in Iran were dedicated to the measurement of ground resistance at various measurement tips moving horizontally through the ground (SHARIFI 2016).

The innovation of the basic study presented here lies in the complete multi-dimensional investigation of the ground resistance distributed over the entire front surface of a cultivator tine and the quantitative identification of highly and low loaded geometry sections for different process parameters.

Reproducible experiments with a homogeneous soil in a soil bin

To investigate the elementary processes between tool and soil, reproducible tests with a sufficient number of repetitions are required. Investigations on natural fields create great measurement uncertainties due to plant residues and vegetation, but also due to the inhomogeneity of the soil type, soil moisture, soil density and the associated soil strength. Homogeneous soil conditions are particularly beneficial for investigation and understanding of sub processes. The measurements were therefore carried out under laboratory conditions in a soil bin without vegetation (soil without humus components) and without sagging or drying effects in the soil. A loamy sand, representative of large parts of the European continent was used as the type of soil. In addition to the advantage of a homogeneous soil structure, a soil bin provides the possibility of adjusting the soil water content. Table 1 lists the measured soil properties of the investigated soil for the respective test settings. The wet bulk density and the water content of the soil in the soil bin were identified as important factors and recorded at certain points between measurements in order to observe changes in the properties of the soil.

Table 1: Measurements, process parameters and soil properties of the analysed data

No.	Measurements		Process parameters (factors)		Soil properties	
	Number of measurement records	Number of evaluated repetitions per measurement record	Levels of working speed in m/s	Levels of the working depth in mm	Water content in % by mass	Wet bulk density in g/cm ³
1	21 (n = 1)	4	0.1 / 0.5 / 1.0 / 1.5 / 2.0 / 2.5 / 3.0	50 / 100 / 150	4.75 (k = 6)	-
2	42 (n = 1)	4	0.1 / 0.5 / 1.0 / 1.5 / 2.0 / 2.5 / 3.0	50 / 100 / 150	3.74 (k = 9)	-
3	12 (n = 2)	5	0.3 / 1.0 / 2.0 / 3.0	100 / 140 / 180	8.16 (k = 12)	1.56 (k = 12)
4	12 (n = 2)	5	0.3 / 1.0 / 2.0 / 3.0	100 / 140 / 180	9.43 (k = 12)	1.59 (k = 12)
5	24 (n = 2)	5	0.3 / 1.0 / 2.0 / 3.0	100 / 140 / 180	4.19 (k = 9)	1.50 (k = 9)
6	24 (n = 2)	5	0.3 / 1.0 / 2.0 / 3.0	100 / 140 / 180	9.98 (k = 12)	1.60 (k = 12)

n: Number of the repetitions of a measurement.

k: Number of soil samples.

In the first two measurements, the gravimetric water content w of the soil was 4.3% on average and can therefore be characterised as dry soil. Whereas the soil of the following four measurements with an average water content of 8.0% can be described as being moist. In addition to the water content, the wet bulk density ρ_F of the soil was measured using a plunging cylinder. After loosening and reconsolidation of the soil, the soil condition encountered to the measuring tine was determined. With regard to the determined wet bulk density of these measurements (1.56 g/cm³), this density, according to SOUCEK et al. (1990), is located in a range that is comparable with natural conditions. Soucek classifies the wet bulk density of sands between 1.3 and 2.0 g/cm³. The range from 1.7 g/cm³ applies to high consolidated or sagged soil properties. The synthetically produced conditions in the soil bin should therefore be regarded as a good approximation of the soil properties occurring in natural environments.

Furthermore, Table 1 shows which process parameters vary as essential factors and in which levels they are divided. In order to be able to identify non-linear effects later, at least three levels were defined per factor. The full-factorial combination of these steps corresponds to the number of measurement records. In measurements No. 3 to 6 (with moist soil), all measurement records were additionally recorded twice (n = 2) in a different test order. The following test results are based on 248 evaluated samples for dry soil and 720 samples for moist soil concerning the number of evaluated repetitions per measurement record.

A total of 14 independent load variables were recorded and evaluated for each measurement record and for each sample within a measurement record. These include on the one hand six load cell forces acting on a measuring frame to determine the total load on the connected tool. On the other hand, eight force signals processed in a piezo-electric measurement chain were recorded for the geometrically discrete evaluation of partial loads with the aid of a measuring tine.

Measuring the total load on a soil tillage tool

A measuring frame is used to measure draught, vertical and lateral forces acting on a rigidly mounted tool. In addition, the torques occurring around all three axes can be determined. This enables to calculate one reduced force vector (wrench in screw theory) out of the load cell forces.

The load measuring frame (also known as dynamometer) used in these studies was designed and manufactured especially for the predicted loads. In principle, this load measuring frame consists of an upper and a lower frame, which are connected to each other via six load cells (Figure 1 a). The load cells have spherical joints at both ends, so that each cell (neglected friction) only transmits tensile or compressive forces and in total all six cells link the upper and lower frame in a mechanically determined manner. The force measuring elements used are strain gauge-based force measuring elements (TECSIS GMBH 2007) with nominal values between $\pm 1,000$ and $\pm 10,000$ N adapted to the installation position. The combined error of the force measuring elements is 0.2% of the full scale value and the time sampling of the connected analogue-to-digital conversion is at 1 kHz.

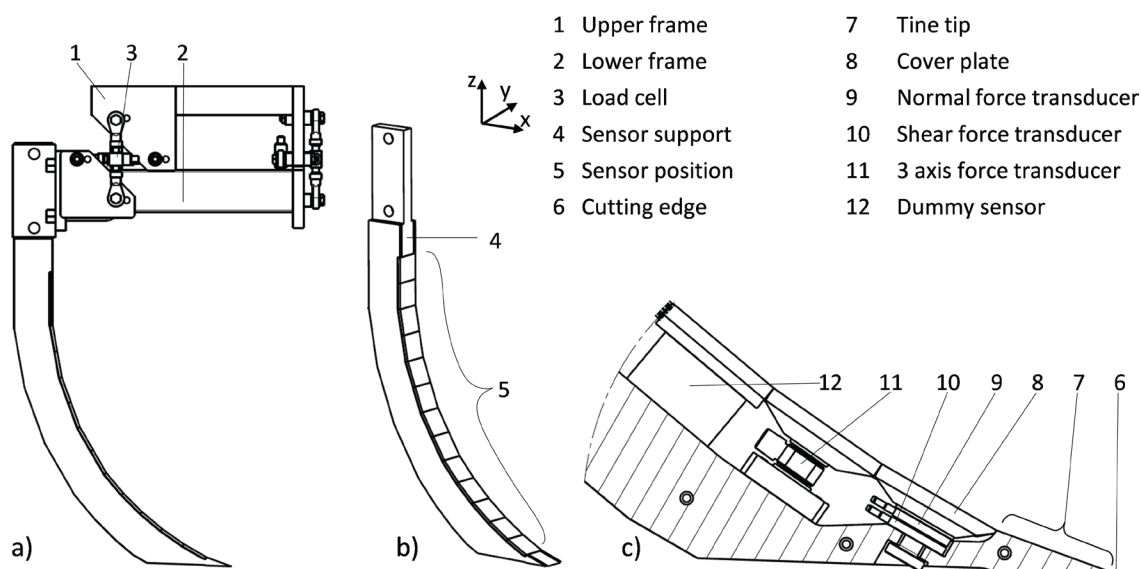


Figure 1: Design of the force measuring elements, a) side view of the load measuring frame and the measuring tine, b) sensor positions of the measuring tine, c) detailed view of the assembly of the tine tip

This information can be used to show the draught force characteristics of the soil tillage implement. The common approaches in literature to describe the draught forces above the working depth or the speed are essentially described by polynomials (ASAE 2003, GORJACKIN 1968). The degree of the polynomials and the value of the coefficients must be determined depending on the tool and soil. Thereby, for instance, different tool geometries can be compared. Another approach was shown by (AL-NEAMA 2017), with an empirical regression model for predicting draft forces using soil mechanics and soil profile evaluation.

Figure 2 shows the draught force acting on the measuring tine in relation to the process parameters tine speed and working depth (hereinafter called draught force characteristic). The measuring tine is shown in the lower right corner. The draught force is applied to the third axis and can be read off in the form of iso-lines of equal draught. The grey dotted field shows the measured values for the

dry soil. The black bordered field shows the draught forces for the moist soil. In both cases an elevation profile is formed, which increases with depth and speed. The gradient of the working depth is greater than the gradient of the tine speed. In addition to the illustration of the parameter ranges investigated in each case, the significant influence of the water content of the soil on the draught forces is evident.

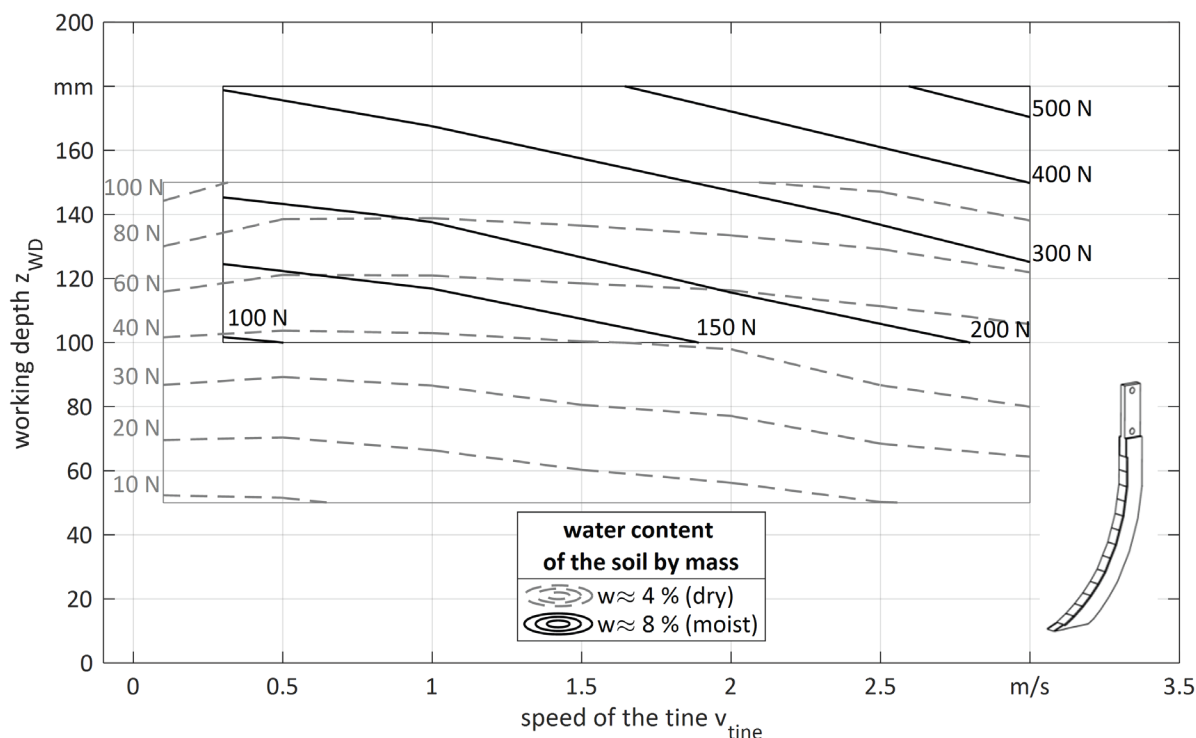


Figure 2: Measured draught force characteristic of the measuring tine for dry and moist soil (loamy sand)

The draught force of the moist soil is above the level for dry soil at all process points. The draught forces for dry soil on the single tine extended over a range of 10 to 120 N. The draught forces of the moist soil are in the range of 100 to 500 N. A comparison with identical process parameters shows that the moist soil has about twice to four times the draught force on the tool. With these observations, there were also considerable differences in the flow and fracture behavior of the soil when increasing the water content of the soil from approx. 4 to 8%. The stronger cohesive forces of the soil lead to higher draught forces on the tool and to larger fragments in the soil structure.

In addition to analysing the draught force characteristic, the load measuring frame is also used as a reference measuring instrument in the context of the discrete load measurement. The reference is thereby the resulting total force vector on the tines. This total force vector can be mathematically calculated as a wrench by the loadcell forces acting vectorially on the measuring frame. The application of this principle to a soil tillage tool is described by RÖHRS und WILKENS (1984). The measuring system used is capable of calculating the direction and magnitude of the resulting force on the tool in all three directions in space (see coordinate system Figure 1 b). Knowledge of the tine geometry and the vector line of the resulting wrench can be used to calculate a point of contact between the force and the tine surface. The following comparison essentially considers the direction and position of the resulting force (wrench).

The measuring tine: A tool for soil tillage for measuring load profiles

The focus of this study is the measurement of normal and shear forces on discrete geometry sections during the tool-soil interaction of a cultivator tine. The development and implementation of this measuring tine was based on proposals (KATTENSTROTH et al. 2015) and findings from a research project funded by the DFG (KATTENSTROTH et al. 2011, HARMS 2010). Production and assembly specifications required the stylization of the tool contour, which was curved in reality. The measuring tine, composed of planar elements, represents a real tool in shape and size (Figure 1).

The measuring tine is designed as a bolted connection of several machined components. Basically, a distinction between the sensor support (4) and the piezoelectric transducers embedded inside it can be made. Behind the cover plates (8), of the 13 discretely distributed sensor positions (5), piezoelectric force transducers (9, 10, 11) or dummy sensors (12) can be mounted. The front surface of the tine, which is formed in the x - z plane, is generated by the flat cover plates in a discontinuous manner, but is very close to a real geometry.

Two 3-axis force measurement transducers type 9017C (KISTLER GRUPPE 2015) were used for the study. Both transducers were preloaded with an expansion bolt between a cover and base plate. These preloaded sensor units can then be installed in the upper 12 sensor positions. The lower sensor position is an exception, as shown in Figure 1c, due to the limited mounting space of the narrowly tapered tip. In order to sense the load as far as possible in the front of the tine geometry, two very flat transducer elements were stacked on top of each other. Using a cover plate (8), a 1-axial compression force transducer (9), type 9015B, and a 1-axial shear force transducer (10), type 9145B, were preloaded directly on the sensor support (4) (KISTLER GRUPPE 2009, 2010) In comparison to the 3-axis transducers, the shear force cannot be measured in the transverse (y) direction. The cover plates of all sensor positions have an identical, flat square surface of 50 x 50 mm². The top side of the tine tip (7), which is equipped without sensors, also follows the stylized discontinuous shape and has these geometric dimensions.

With this measuring instrument, sensor positions 2 to 7 for dry soil and sensor positions 1 to 7 for moist soil were measured. Since the positions 2 to 7 must be occupied by the two 3-axis force transducers, there are three installation states for complete coverage. The process parameters described in Table 1 were then set for each of the three installation states. The following illustrations thus always show the loads superpositioned from three measurements of the measuring tine.

Since a geometrically fixed sensor operates at different effective depths with different process parameters or experiences a different inflow, a geometrically fixed tine coordinate system and a ground fixed soil coordinate system are to be introduced first. Figure 3 a shows the tine coordinate z_{tine} , which is fixed vertically to geometry at the cutting edge and points upwards. The graphic shows a simplified flow of the soil passing along the tine. At the level of the ground surface the working depth z_{WD} is shown. Starting from the ground surface and also positively aligned vertically, the ground fixed coordinate z_{Ground} is defined. The numbering of the sensor positions starts at the tine tip with $P = 1$ and also increases in the z direction to $P = 13$. The normal and shear forces acting on the transducers correspond to the respective normal stress p_N and the tangentially acting shear stress p_S , relative to the surface of the cover plate (Figure 3 b).

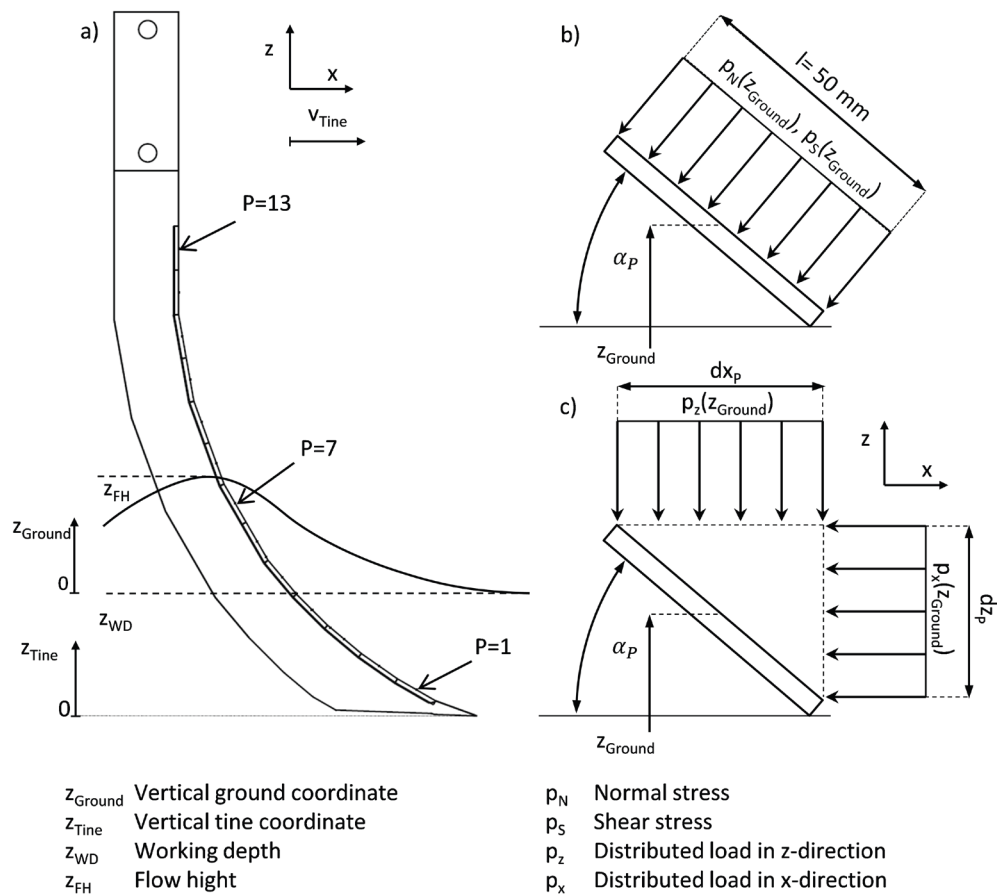


Figure 3: a) Geometry and ground fixed coordinate system, b) Normal and shear stress on the cover plates, c) Vertical and horizontal distributed load on the cover plate

Figure 4 shows normal stress and shear stress profiles for the working depth $z_{WD} = 180$ mm in moist soil. It can be observed that both the normal stress and the shear stress do not extend evenly along the depth z_{Ground} . It turns out that the stresses in the normal and shear directions increase with increasing depth and that the largest measured values occur at $z_{Ground} = -150$ mm. Looking at the drawn curves shows that this load distribution can be observed similarly at different tine speeds. The position of the load profiles as a function of the tine speed v_{Tine} can be read off from the plotted set of curves. Like the forces on the entire tool, the loads on individual geometry sections increase with increasing speed. The figure shows the increasing load on the cultivator tine, in the direction of the tool tip, and how this distribution is expressed quantitatively as a function of the speed of the tine. These observations also correspond qualitatively to the theoretical forces of soil reactance on a curved plane determined for a two-dimensional case by (SÖHNE 1956).

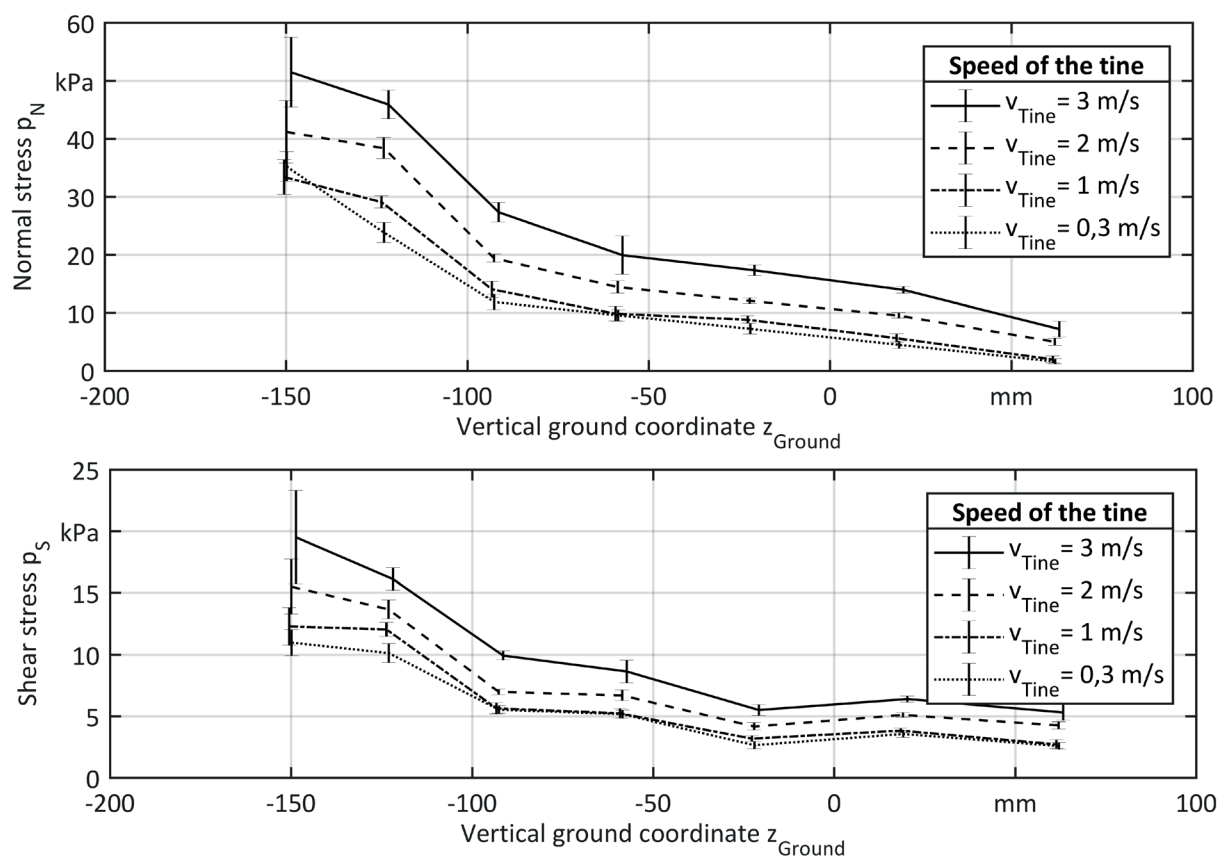


Figure 4: Load profiles as normal and shear stress profiles of different tine speeds v_{Tine} for moist soil at a working depth $z_{WD} = 180$ mm

The displayed error bars in the load profiles show the determined standard deviation ($\pm \sigma$) of the measured values. These uncertainties can be explained by different causes: Variation in working operating depth, differences in water content in the soil and thus changes in soil cohesion, fluctuations in wet bulk density and systematic errors during the installation and calibration of the individual sensors. Another aspect is the breaking up of cohesive soil. Since cohesive soil fractures to soil blocks, the loading of the tool follows the periodic breaking and sliding of the soil blocks. This periodicity was averaged over time in these measurements.

Since the measurements are based on a high number of data points, a suitable statistical certainty can be assumed. Following, a further analysis and a comparison of the partial loads and the total forces measured on the load measuring frame will be shown.

Summation of partial forces to resulting tool loads

A summation of all applied partial forces (loads) on the tool surface must correspond to the total force acting on the tool. Two circumstances must be noted when applying such an approach to the measurement results shown. The partial loads are always summed up for a constant process point, consisting of tine speed and working depth. This is to be mentioned in particular due to the superposition of the partial forces. In addition, not all partial forces acting on the surface can be detected individually with the present measuring tine.

In order to be able to sum up the partial forces of a process point, it is necessary to transform the forces acting normally and tangentially on the cover plates into a common coordinate system. The transformation is done by rotating around angle α_P at each position P and moving in the global x, y, z geometry coordinates (Figure 3 b). The area centres of the cover plates serve as location vectors. Figure 5 a shows these measured partial forces in vectorial representation above the tine geometry at a working depth of $z_{WD} = 180$ mm and a speed of $v_{Tine} = 2$ m/s in moist soil.

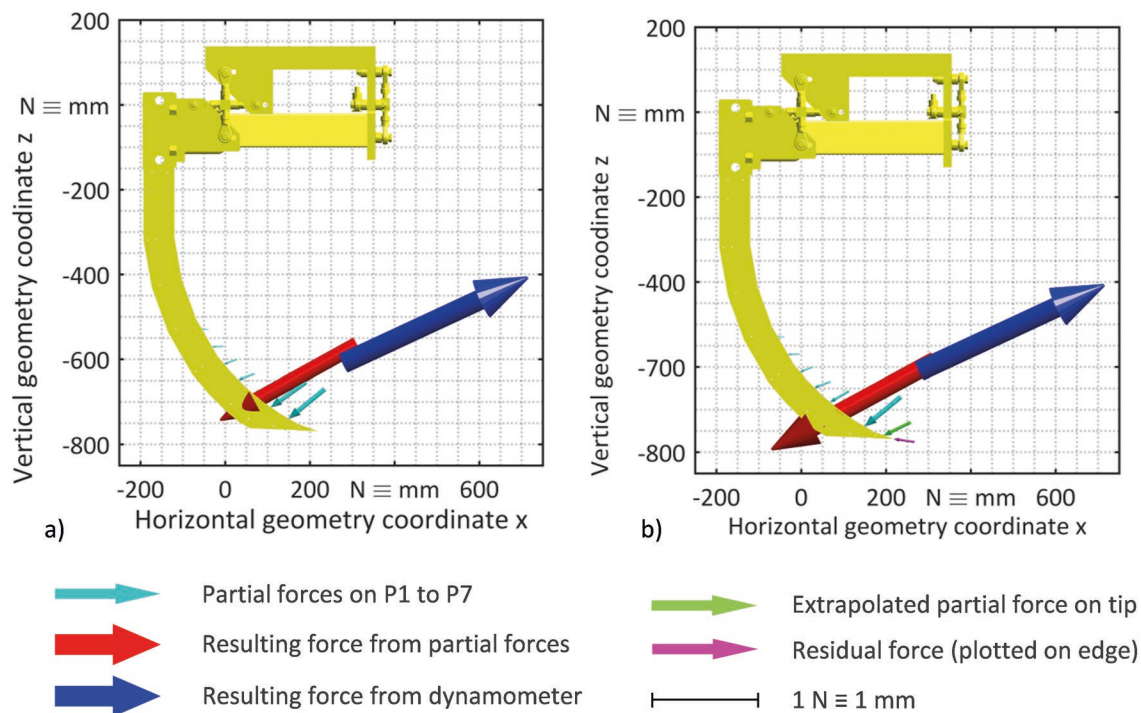


Figure 5: Load on the measuring tine for moist soil at a working depth $z_{WD} = 180$ mm and a working speed $v_{Tine} = 2$ m/s, a) Measured forces on the load measuring frame and the measuring tine, b) Extrapolated load profile of the measuring tine taking into account the forces not detected at the top of the point.

All force vectors illustrated as arrows are scaled with $1 \text{ N} \cong 1 \text{ mm}$. The cyan coloured shorter arrows are the measured partial forces. Moreover, a resulting force was calculated from these partial forces, which is represented by the red arrow. As reference, the force calculated from the load cell forces acting on the load measuring frame is shown in blue. This resulting load is directed in the opposite direction to the force of the partial loads. The resulting vector lines of both forces are approx. 50 mm apart at the tool surface. A comparison of these vector lengths shows a force difference (or residual force) between the measurement at the measuring tine and the measurement at the force measuring frame for all process parameters. In the case shown, the force difference is 114 N (24% of the resulting total force). Since the resulting force of the partial loads is smaller than the resulting force of the load measuring frame, it is assumed that this difference is due to the forces not recorded.

The following assumptions and explanations will be used to estimate the forces not measured: Due to an ideal, symmetrical soil flow, no resulting forces occur in the transverse direction. Friction on the side surfaces of the tool is neglected. The essential load (not measured) is above the tine tip (7) shown in Figure 1 c or on the cutting edge (6).

To calculate the forces acting on the top of the point, the measured loads are extrapolated. It is assumed that the load continues in the direction of the peak. The following extrapolation has been applied. The measured normal and shear forces are divided into horizontal and vertical components by the angle α_p . This corresponds to the procedure mentioned above for summing up and calculating the resulting force. For extrapolation, the forces are now converted into distributed loads in the x and z directions. The forces are referred to the projection surface in the x- and z-direction (Figure 3 c). Since the angle α_p become flatter towards the tip, this results in a kind of weighting of the load for both directions. Figure 6 shows the distributed loads p_x and p_z above the vertical ground coordinate z_{Ground} for the process point shown above.

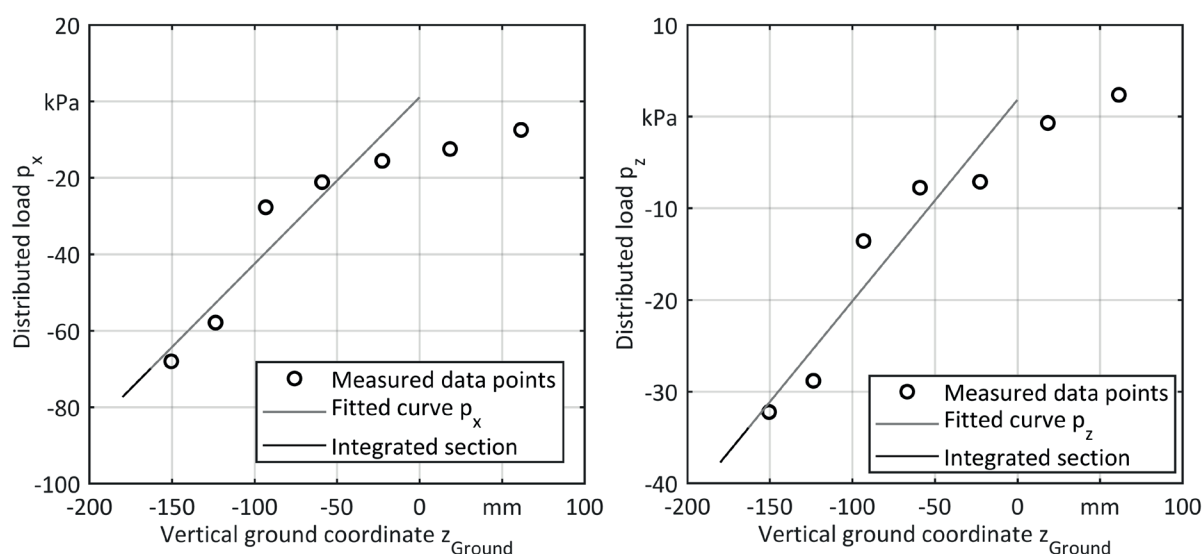


Figure 6: Horizontal and vertical distributed loads p_x and p_z for moist soil at an working depth $z_{WD} = 180$ mm and an tine speed $v_{Tine} = 2$ m/s

According to the investigations of SHARIFI (2016) with a measuring tool consisting of horizontally arranged penetrometers, it should be assumed that the pressure in the direction of travel (p_x) is linear with the depth z_{Ground} . Likewise, the vertically loading pressure should be assumed to increase linearly. Both linear curves should only count below the soil surface, for $z_{Ground} < 0$. The linear fitted lines are shown in Figure 6 next to the measured data points. Now it is possible to integrate these determined linear relationships $p_x(z_{Ground})$ and $p_z(z_{Ground})$ via z_{Ground} within the effective depth of the tine tip (here: -162.9 mm to -180 mm). Multiplied by the constant tine width $b = 50$ mm, the forces F_x and F_z result on the upper side of the tine tip:

$$F_x = b \cdot \int_{z=-162.9}^{z=-180} p_x(z_{Ground}) dz$$

$$F_z = b \cdot \int_{z=-162.9}^{z=-180} p_z(z_{Ground}) dz$$

The green arrow in Figure 5 b shows these extrapolated force components applied to the area center of the point. Taking this extrapolated vector into account, a new resultant load of the measuring tine is created, the force vector shown in Figure 5 b in red. It can now be seen that the vector lines of the resulting force of the load measuring frame and the measuring tine are closer to each other and that the length of the vectors also better match. In this example, the magnitude of the resulting vectors (residual force) in the x-z plane differs by only 49 N (10% of the resulting total force). The distance between the vector lines at the tool surface is approx. 10 mm.

The remaining residual force (differences between the total force generated by the extrapolated load profile and the total force of the load measuring frame in x-z plane) can be explained by the fact that the measurement uncertainties increase significantly at low forces and that the geometric surfaces described earlier are not taken into account. Table 2 gives an overview of the absolute and relative residual force.

Table 2: Absolute and relative residual force with extrapolation of the load profile

		Speed of the tine in m/s			
		0.3	1	2	3
Working depth in mm	100	29 N (29%)	23 N (21%)	28 N (17%)	34 N (15%)
	140	40 N (21%)	39 N (18%)	45 N (15%)	48 N (13%)
	180	42 N (12%)	43 N (12%)	49 N (10%)	50 N (8%)

Absolute residual force: Amount of residual force in the x-z plane.

Relative residual force: Amount of the residual force to the amount of the total force in percentage of reference (the load measuring frame) in the x-z plane.

An examination of the residual force without extrapolation shows values between 38 and 130 N or between 21 and 40% of the total force. It can be seen that the extrapolation results in consistently lower residual forces. An examination of the residual forces including the extrapolated force component at the top of the point shows the following picture: The residual force lies in a range between 23 and 50 N. This corresponds to relative values of 8 to 29% of the total force. The residual force is greater for small process parameters (low working depth and slow tine speed) than for higher values of the process parameters. The measured forces at low working depths and speeds are at the lower end of the sensor measuring range and also below the usual process-related speed values.

The goal of a complete, geometric discrete load analysis and the determination of load profiles over the tool geometry is achieved differently well with different process parameters.

Conclusions

The measuring device used in the presented study to determine geometric discrete loads and load profiles on a soil tillage tool during soil interaction represents an innovation for the methods known so far in science and technology. It was possible to show qualitatively and quantitatively how normal and shear stresses develop over the tine geometry. As a result, the load profiles for the process parameters tine speed and working depth are determined for two water contents of the soil. The method and the collected data serve as an important basis for research into the design of soil tillage tools. These findings are of particular interest with regard to the further development and analyses with DEM simulation methods. For the parameterization of soil models and not least for the validation of simulation results, the measurement technology and the results obtained can be accessed.

References

- Al-Neama, A. K. A.; Herlitzius, T. (2017): Draft forces prediction model for standard single tines by using principles of soil mechanics and soil profile evaluation. *Landtechnik* 72(3), <http://dx.doi.org/10.15150/lt.2017.3161>
- American Society of Agricultural Engineers ASAE (2003): ASAE Standards 2003 (ASAE D497.4), ASAE D497.4, pp. 372–380
- Djatschenko, G. (1972): Zur Untersuchung des Scharschneidenwinkels von Grubberwerkzeugen für hohe Arbeitsgeschwindigkeiten. *Deutsche Agrartechnik* 22(1), S. 22–25
- Gorjackin, W. P. (1968): *Sobranie socinenij. Gesammelte Werke, Bd. 2.* Moskau, Verlag Kolos
- Harms, H.-H. (2010): Reibkraftreduzierung durch hochfrequente Schwingungsanregung am Beispiel der Bodenbearbeitung. Projektnr. 83596685, DFG-Abschlussbericht HA 1100/36-1
- Kattenstroth, R.; Harms, H.-H.; Wallaschek, J. (2015): Hochfrequente Werkzeugschwingung zur Zugkraftreduktion bei der Bodenbearbeitung. Dissertation, Technische Universität Braunschweig, Shaker Verlag GmbH
- Kattenstroth, R.; Harms, H.-H.; Lang, T.; Wurpts, W.; Twiefel, J.; Wallaschek, J. (2011): Reibkraftreduktion mittels Ultraschallanregung in der Bodenbearbeitung. *Landtechnik* 66(1), <https://doi.org/10.15150/lt.2011.341>
- Kistler Gruppe (2009): Betriebsanleitung, Typ 9135B21. SlimLine Sensoren (SLS) Typ 9130B... bis 9137B
- Kistler Gruppe (2010): Betriebsanleitung, Typ 9145B21. SlimLine Sensoren (SLS) Schubkraft Typ 9143B... bis 9147B
- Kistler Gruppe (2015): Betriebsanleitung, Typ 9017C. Piezoelektrischer 3-Komponenten- Kraftsensor Typ 9017C, 9018C, 3-Komponenten- Kraftsensor Typen 9027C, 9016C4
- Mattetti, M.; Varani, M.; Molari, G. (2015): Measurement of the soil pressure on a plough. In: *Land.Technik AgEng 2015, 73rd International Conference on Agricultural Engineering „innovations in agricultural engineering for efficient farming“* in Hannover, 06–07 November 2015, Düsseldorf, VDI-Verl., pp. 487–491
- Röhrs, W.; Wilkens, D. (1984): Kraftmessungen an Bodenbearbeitungsgeräten. *Grundlagen der Landtechnik* 34(3), S. 117–125
- Sharifi (2016): Comparison of cone and prismatic tips for measuring soil mechanical resistance by a horizontal sensor. *CIGR Journal* 18(2), pp. 66–72
- Siemens, J. C.; Weber, J. A.; Thornburn, T. H. (1965): Mechanics of Soil as Influenced by Model Tillage Tools. *Transactions of the ASAE* 8(1), pp. 1–7, <https://doi.org/10.13031/2013.40412>
- Söhne, W. (1956): Einige Grundlagen für die Landtechnische Bodenmechanik. *Grundlagen der Landtechnik – Konstruktiveurhefte* 7, S. 11–27
- Soucek, R.; Pippig, G. (1990): *Maschinen und Geräte für Bodenbearbeitung, Düngung und Aussaat.* Berlin, Verlag Technik
- tecsis GmbH (2007): Betriebsanleitung Zug-/Druckkraftaufnehmer F2301/F23C1. Offenbach am Main, tecsis GmbH
- Ucgul, M.; Fielke, J. M.; Saunders, C. (2014): 3D DEM tillage simulation. Validation of a hysteretic spring (plastic) contact model for a sweep tool operating in a cohesionless soil. *Soil and Tillage Research* 144, pp. 220–227, <https://doi.org/10.1016/j.still.2013.10.003>
- Vornkahl, W. (1967): Beitrag zur Gestaltung von zinkenartigen Bodenbearbeitungswerkzeugen. *Grundlagen der Landtechnik* 17(3), S. 95–98

Authors

Johannes Bührke (M.Sc.) and **Florian Schramm (M.Sc.)** are research assistants and **Prof. Dr. Ludger Frerichs** is the director of the Institute of Mobile Machines and Commercial Vehicles at Technische Universität Braunschweig, Langer Kamp 19a, 38106 Braunschweig, e-mail: johannes.buehrke@tu-braunschweig.de.

Acknowledgements

The project was financially funded by the German Research Foundation (DFG).